Packed modulation loops to reduce band broadening in two-dimensional liquid chromatography

Knol, W.C.; Peters, R.A.H.; Pirok, B.W.J.

DOI
10.1016/j.chroma.2023.463802

Publication date
2023

Document Version
Final published version

Published in
Journal of Chromatography A

Journal of Chromatography A 1690 (2023) 463802

Contents lists available at ScienceDirect

Journal of Chromatography A

journal homepage: www.elsevier.com/locate/chroma

Packed modulation loops to reduce band broadening in two-dimensional liquid chromatography

Wouter C. Knol[a,b,*], Ron A.H. Peters[a,b,c], Bob W.J. Pirok[a,b]

[a] Analytical Chemistry Group, van 't Hoff Institute for Molecular Sciences (HIMS), Faculty of Science, University of Amsterdam, Science park 904, Amsterdam, the Netherlands
[b] Centre for Analytical Sciences Amsterdam, Science park 904, Amsterdam, the Netherlands
[c] Covestro, Group Innovation, Sluisweg 12, Waalwijk, the Netherlands

ARTICLE INFO

Article history:
Received 18 November 2022
Revised 12 January 2023
Accepted 13 January 2023
Available online 14 January 2023

Keywords:
Modulation
Dispersion
Packed loops
Elution profiles
Two-dimensional liquid chromatography

ABSTRACT

Modulation interfaces employing sample loops are applied in many hyphenated separations such as two-dimensional liquid chromatography (2D-LC). When the first-dimension effluent in 2D-LC is eluted from the modulation loop, dispersion effects occur due to differences in the laminar flow velocity of the filling and emptying flow. These effects were recently studied by Moussa et al. whom recommended the use of coiled loops to promote radial diffusion and reduce this effect. In the 1980s, Coq et al. investigated the use of packed loops, which also promote radial diffusion, in large volume injection 1D-LC. Unfortunately, this concept was never investigated in the context of 2D-LC modulation. Our work evaluates use of packed loops in 2D-LC modulation and compares them to unpacked coiled and uncoiled modulation loops. The effect of the solvents, loop volume, differences in filling and emptying rates, and loop elution direction on the elution profile was investigated. Statistical moments were used as a pragmatic tool to quantify elution profile characteristics. Decreased dispersion was observed in all cases for the packed loops compared to unpacked loops and unpacked coiled loops. In particular for larger loop volumes the dispersion was reduced significantly. Furthermore, countercurrent elution resulted in narrower elution profiles in all cases compared to concurrent elution. We found that packed modulation loops are of high interested when analytes are not refocussed in the second-dimension separation (e.g. for size-exclusion chromatography). Moreover, our work suggests that the use of packed loops may aid in prevention of loop overfilling.

1. Introduction

Modulation interfaces are applied in many hyphenated analytical separation workflows to transfer the effluent from the first dimension to the second. In chromatography this is particularly common in two-dimensional liquid chromatography (2D-LC). In comprehensive two-dimensional liquid chromatography (LC × LC) two modulation loops (capillaries with a set volume) are used (Fig. 1) alternatingly to ensure that all effluent eluting from the first-dimension (^{1}D) column can be injected into a second-dimension (^{2}D) column [1].

Since the modulation loop is typically emptied at a higher flow rate than it is filled, dispersion of the analyte plug occurs during the elution of the loop [2]. This is of little concern in applications using RPLC, or other separation modes where analytes are refocussed at the column head, in the ^{2}D. In applications where analytes are not refocussed in the ^{2}D dimension or where the effective volume of the ^{1}D eluent plug must be constrained, this issue is problematic. For example, in active solvent modulation LC × LC and in In-Line Mixing Modulation LC × LC this dispersion will lead to a longer required time to fully empty the loop, which could result in a longer ^{2}D analysis time [3,4]. In heart-cut 2D-LC it will also affect the ^{2}D injection profile resulting in deformed peaks if no refocussing in the ^{2}D analysis is achieved. Even in more exotic hyphenations, such as LC-GC, the increased total volume of eluent needed to fully displace the loop contents might be problematic, as larger volume injections are required to inject all fractionated effluent [5,6]. The aforementioned dispersion yields a non-symmetrical and broad elution profiles when modulation loops are emptied at higher rates than they are filled [2]. This effect also occurs during injection 1D-LC and has been extensively studied [7,8]. Moussa et al. recently described this issue

* Corresponding author.
E-mail address: W.C.Knol@uva.nl (W.C. Knol).

https://doi.org/10.1016/j.chroma.2023.463802

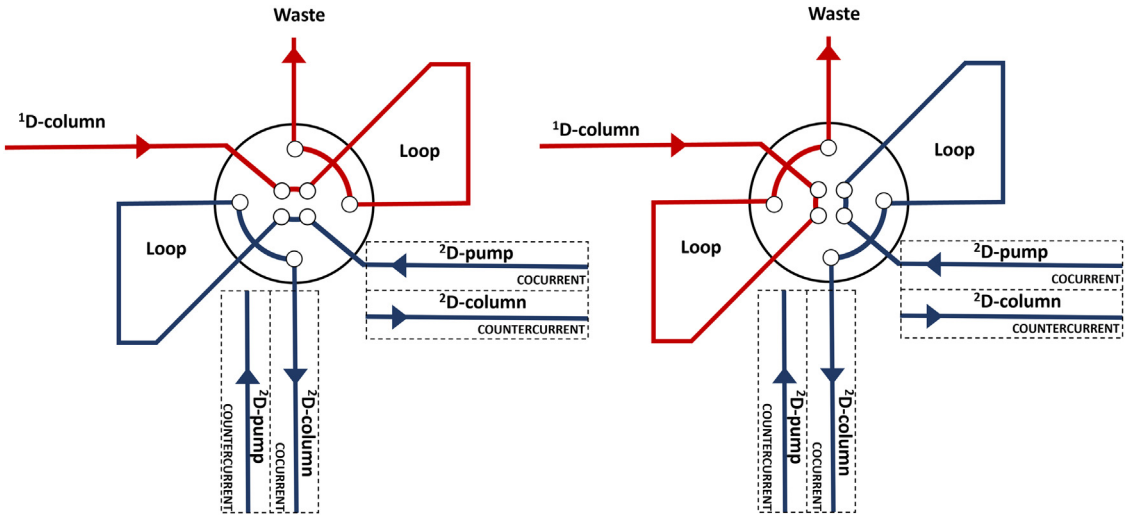

Fig. 1. Example of a passive modulation 2D-LC configuration, in both valve positions, here depicted in both counter and cocurrent elution mode.

fundamentally in 2D-LC modulation and recommended the use of coiled modulation loops to limit this effect [2]. The dispersion is limited by radial diffusion, as it promotes migration between the differing flow velocities across the radial plane of the loop [8]. The promotion of radial diffusion thus limits the observed dispersion [9,10]. Practically, this can be achieved by coiling the loops, which induces centrifugal flows and thus promotes radial mixing [2]. In theory the packing of the loop with an inert material should also reduce the dispersion, as the packing material will introduce eddy diffusion which promotes mixing in the radial dimension and thus reduces dispersion. In essence, the goal is to limit the spread in the velocity across the analyte molecules in the loop.

Interestingly, this concept was already investigated in the 1980's by Coq et al. for large volume injection in conventional LC [11]. The authors theoretically investigated the advantages and disadvantages of using packed injection loops for very large (V_{inj} > 500 μL) injection volumes and included the pressure drop across the loop volume in their assessment. The authors considered three injection loop configurations (i) continuously in-line injection with empty loops, i.e. the sample loop is always in-line with the flow for the duration of the entire experiment, (ii) bringing the injection loop in-line only for one loop volume, and (iii) the use of a loop packed with glass-beads. For the empty loop case (i), the authors concluded that the loops should be narrow and coiled. For case (ii), increased dispersion was observed but the authors were concerned about the precision of the valve switches as well as pump accuracy. Finally, for case (iii), the authors concluded that packed loops yielded minimized band broadening, yet also expressed concerns about the pressure drop along the packed loop. This last concern might be less relevant in 2D-LC as pumps are used for filling the loops. Furthermore, an attractive property of packed loops in 2D-LC that is not relevant in 1D-LC, may be the reduction of overfilling [12,13]. The pressure-driven parabolic flow profile renders overfilling a significant risk (see Supplementary Materials Figure S-1 for a simulated example). Packing the loops promotes radial diffusion, allowing the loop to be filled further without risking sample loss.

Given that all LC separations employ empty loops for injection, it is surprising that the work of Coq et al. never gained traction in particular for 2D-LC separations. In LC × LC, the loop is typically not fully filled and the concentration over the loops is thus not homogenous [2]. The optimal elution shape, for a loop filled a homogenous concentration, features a perfect block profile. This theoretical optimum for the variance introduced by the injection can also be expressed mathematically (Eq. (1)) by the second statistical moment for the block profile.

$$\sigma^2_{V,inj} = \frac{V_i^2}{12} \tag{1}$$

In which $\sigma^2_{V,inj}$ is the variance induced by the injection and V_i is the injection volume. Of course, in practice, (i) loops are not homogenously filled, as analyte concentration in the ^{1}D eluent varies over the run, and (ii) contributions by the multiple extra-column components (i.e. tubing, connections, etc.) are not negligible. This is especially true for the case of 2D-LC where modulation volumes are small (typically in the range of 20–60 µL) [13]. It is thus not reasonable to expect a perfect block profile such as described by Eq. (1), yet still it is useful as it provides a point of reference.

An approach to quantify peak characteristics are statistical moments, which describe the actual shape of the peak and thus offer a good description of the total elution profile [14,15]. The zeroth moment (M_0, Eq. (2)), describes the area of the peak.

$$M_0 = \int_a^b f(t)dt \tag{2}$$

In which the peak is expressed as distribution $f(t)$ over time t, a and b are the start and end points of the peak. This immediately raises the main disadvantage of using statistical moments to describe chromatographic peaks, as an accurate determination of the start and end point of a peak may be challenging in case of complex baseline deformations and co-elution. Therefore, the use of statical moments suffices for the present study as they are only applied to describe elution profiles where the start and end points could be accurately determined. The first moment (M_1, Eq. (3)) can also be calculated, but must be normalized by the area (M_0) to yield the normalized first moment (m_1, Eq. (4)) which presents the mean retention time.

$$M_1 = \int_a^b t \cdot f(t)dt \tag{3}$$

$$m_1 = \frac{\int_a^b t \cdot f(t)dt}{M_0} \tag{4}$$

Further statistical moments of interest must be centralized using the normalized first moment. Eq. (5) can then be used to calculate the centralized second moment (μ_2), which represents the variance σ^2, as well as the skew (S, i.e. asymmetry, Eq. (6)) and kurtosis (K, Eq. (7)).

$$\mu_n = \frac{\int_a^b (t - m_1)^n f(t)\, dt}{M_0} \tag{5}$$

$$S = \frac{\mu_3}{\sigma^3} \quad (6)$$

$$K = \frac{\mu_4}{\sigma^4} \quad (7)$$

The kurtosis is a measure of the compression or stretching of the peak along a vertical axis. It can be visualized by moving in, or pulling apart, the sides of a Gaussian distribution while maintaining a constant area. A kurtosis value of 1.8 represents a block shape. Various distributions along with their respective K value are depicted in Supplementary Materials Figure S-2.

Coq et al. found significant reductions the injection elution band width when using coiled and packed loops in large volume injection in 1D-LC [11]. Moussa et al. performed computational modelling of elution profiles during modulation in 2D-LC and recommended the use of coiled loops [2]. However, the work of Moussa et al. did not investigate packed loops as introduced by Coq et al. in 1D-LC injection. Its implementation also has thus not been considered for 2D-LC, where the difference between injection and filling rates and direction is significant.

In this work, we aim to experimentally investigate the feasibility of using packed loops to limit band broadening during modulation in 2D-LC. We expand on the findings by Coq et al. and Moussa et al. and now focus on factors relevant for 2D-LC including the use of cocurrent and countercurrent elution (also called forward-flush or concurrent and backflush elution respectively), as well as the applicability for small and large molecules (i.e. polymers). We use statistical moments as a simple tool to characterize elution profiles and to compare the use of empty loops, coiled empty loops, and packed non-coiled loops, for different loop volumes and solvents (aqueous or organic). The term “packed loops” should not be confused with the use of retention-facilitating packed columns in active modulation that are sometimes employed in 2D-LC, such trapping mechanisms are out of the scope of this study.

2. Materials and methods

2.1. Loop preparation

2.1.1. Packed loops

Packed loops were prepared by filling 1 mm i.d. tubing (BGB Analytik, Harderwijk, The Netherlands) with 20 µm monodisperse silica particles (Sigma Aldrich, Darmstadt, Germany). Inline filters were used to act as a frit to retain the packing. Packing was performed by placing an inline filter on one end of the desired length of 1 mm i.d. tube. This end of the tubing was placed in a beaker and placed in an ultrasonic bath to transfer vibrations to the tube during packing. The tube was then manually filled trough a narrow funnel until it was visually confirmed to be fully filled and no additional settling of the stationary phase was observed upon introducing additional vibrations upon tapping the tube with a spatula.

For the 40 µL loops, 12.7 cm of 1 mm i.d. tubing was packed and 0.2 µL internal volume ACQUITY Column In-Line Filters (Waters, Milford, PA, USA) with 0.2 µm frits were used to retain the packing. For the 100 µL loops, 31.8 cm of 1 mm i.d. tubing was packed and Agilent inline filters with a 0.2 µm frits (Agilent, Waldbronn, Germany, Part Number:5067–1551) were used to retain the packing. To connect the 100 µl packed loop to the valve 7 cm of 0.12 mm i.d. tubing (0.8 µL) was used. Note that the loop volume is expressed as the liquid accessible volume (i.e. the exclusion volume, excluding the solid-particle volume), estimated as 40% of the total loop volume, as the theoretical optimum is 36.5% [16].

2.1.2. Non-packed loops

As an empty reference loop, one Agilent 40 µL 2D-LC loop (i.d. 0.25 mm, length ± 81.5 cm, Part Number:5067–5425) was used. One additional such loop was coiled around a tube yielding a total of 10 coils with a ± 2.5 cm i.d. A piece of 50 cm of 0.5 mm i.d. tubing (Agilent, 98.2 µL) was used to compare to the 100 µL packed loop. The coiled 100 µL loop, made of an additional piece of such tubing, consisted of 7 coils with an i.d. of ±2.5 cm.

The volumes of the loops were confirmed using injections with dead-volume markers. For this 20 µL of a 0.05 mg·mL^{-1} 4–hydroxyphenylacetic acid (Sigma Aldrich, Darmstadt, Germany) solution in water was injected with a flow of 0.1 mL·min^{-1}. The used system is described in *Section 2.2*. For the dead-volume measurements the modulation loop was kept in line for the entire experiment. Loop volumes were compared relatively to commercial variants. Based on triplicate measurements the 40 µL packed loop was 2.7 µL smaller in volume than the unpacked commercial equivalent, which can likely be attributed to inaccuracy in the fabrication. The 100 µL packed loop was found to have a volume 7.4 µL larger than the tubing (50 cm × 0.5 mm i.d.) it was compared to, which can be attributed to non-optimal packing. Photographs of the loops applied in the study are featured in Supplementary Materials Figure S-3.

2.2. Aqueous experiments

A solution of 0.05 mg·mL^{-1} 4–hydroxyphenylacetic acid (Sigma Aldrich, Darmstadt) was prepared in demineralized water. The used LC system consisted of two Agilent 1290 Infinity II binary LC pumps (G7120A), an Agilent 1290 Infinity II diode array detector (G7117B) and autosampler (G7129B). An Agilent 1100 column compartment (G1316A) with a 6-port valve was used to fill and empty the loops. Detection was performed at a wavelength of 254 nm and an acquisition rate of 20 Hz. The loops were filled with the 4–hydroxy phenol acetic acid solution at a rate of 10 µL·min^{-1}, for various durations after which the valve was switched to elute the loop at flow rate of 1, 0.1, 0.05 or 0.01 mL·min^{-1} with demineralized water. A schematic representation of the configuration used for testing the loops is given in Fig. 2.

2.3. Organic experiments

Solutions of polystyrene standards (Polymer Labs, Church Stretton, Shropshire, UK) of differing molar masses (980, 9920, 96,000 and 1,112,000 Da) were prepared in unstabilized THF (VWR, Amsterdam, The Netherlands) at a concentration of 0.05 mg·mL^{-1}. Toluene (VWR) was taken as a low molar mass reference. The LC system consisted of an Agilent 1100 binary pump (G1312A), an Agilent 1260 nano pump (G2226A), which was used for filling the loops, and an Agilent 1100 UV detector (G1315B) and autosampler (G1329B). The loops were filled with the polystyrene or toluene solution at a rate of 10 µL·min^{-1} for 2 min after which the valve was switched to elute the loop at 1 mL·min^{-1} with unstabilized THF.

3.Results and discussion

3.1 Loop characterization and performance

There are two main elution modes that are applied in 2D-LC: cocurrent and countercurrent elution. In the former, the loops are emptied in the same direction they are filled; in the latter, the loop contents are emptied in the opposite direction. Fig. 3 shows the comparison of experimental elution profiles between non-packed non-coiled, non-packed coiled and packed loops (non-coiled), filled for 50% at 10 µL·min^{-1} and eluted at 1 mL·min^{-1} (*Section 2.2* for exact conditions). A higher elution than filling flow is common in 2D-LC (especially in LC × LC) as the ^{2}D separation is generally performed much faster than the ^{1}D separation. Figs. 3A and 3C

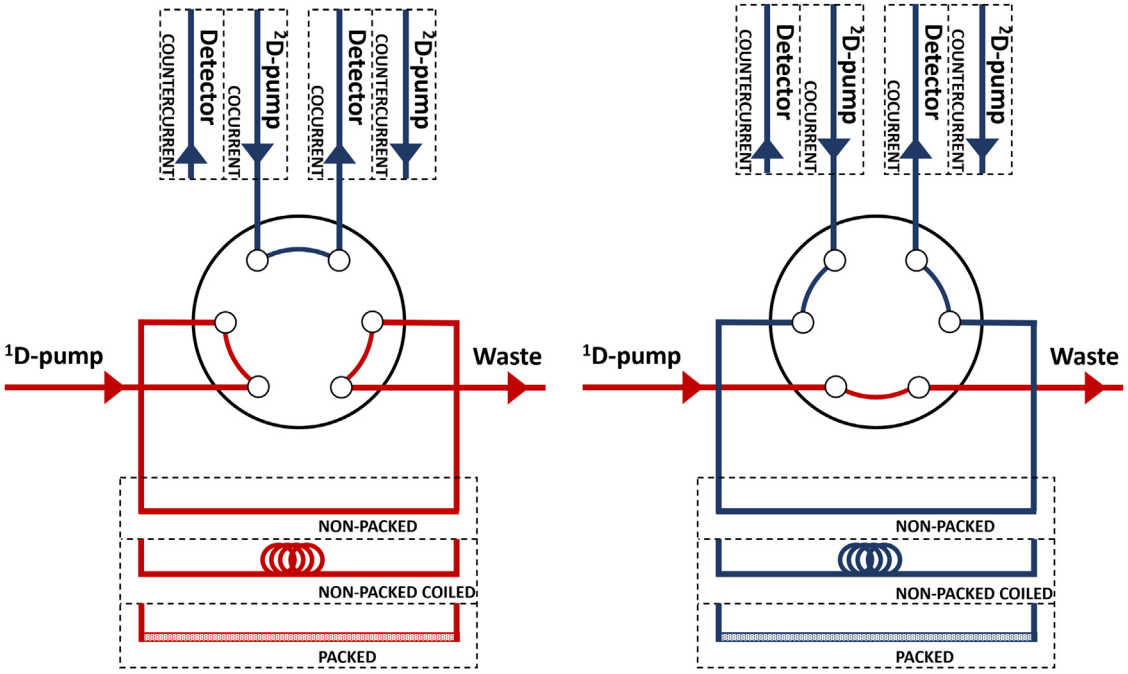

Fig. 2. Schematic representation of the experiential setup in the loop filling and emptying valve position.

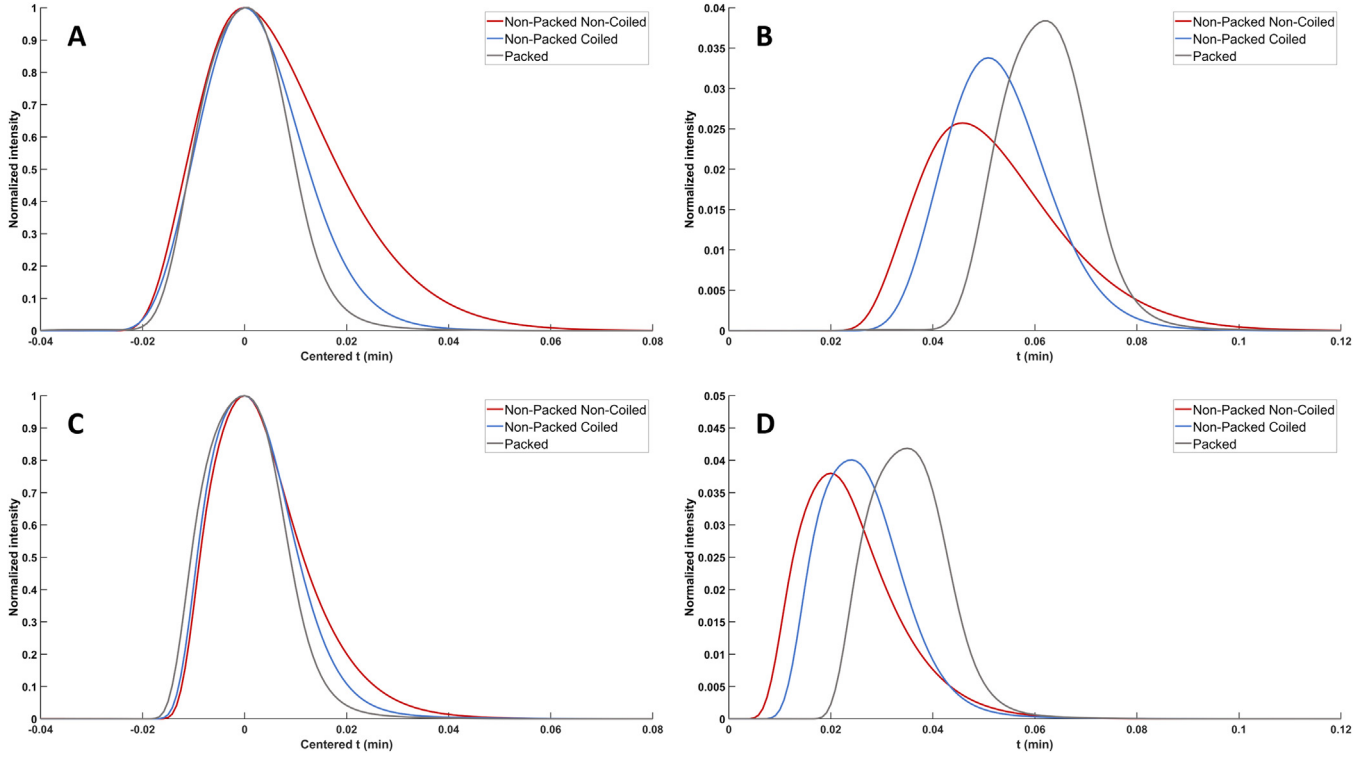

Fig. 3. Average ($n = 3$) elution profiles of non-packed non-coiled (red), non-packed coiled (blue) and packed loops (grey) in cocurrent (panel A,B) and countercurrent (C,D) elution mode both centred and normalized to the peak maximum (A,C) and only normalized to the peak area (C,D).

show the obtained elution profiles, with elution times centred to the peak apex and signals normalized to the peak maximum.

To compare the average elution speed, elution profiles normalized to their total area are also shown (Fig. 3B and 3D). The width of the elution profile for the non-packed non-coiled loop is the largest, which is in agreement with the findings of Coq et al. [11]. Coiling the loop reduces the peak asymmetry drastically, packing the loops offers the least dispersion because it induces the most radial mixing. In all cases, cocurrent elution (Fig. 3A-B) yielded broader and more asymmetrical peak shapes than countercurrent elution (Fig. 3C-D).

Figs. 3B and 3D also show that the analytes in the packed columns elute later, which can be attributed to the average analyte velocity being lower due to more radial mixing. However, the distribution in their elution distance was narrower, thus leading to sharper elution bands. This supports our hypothesis regarding the

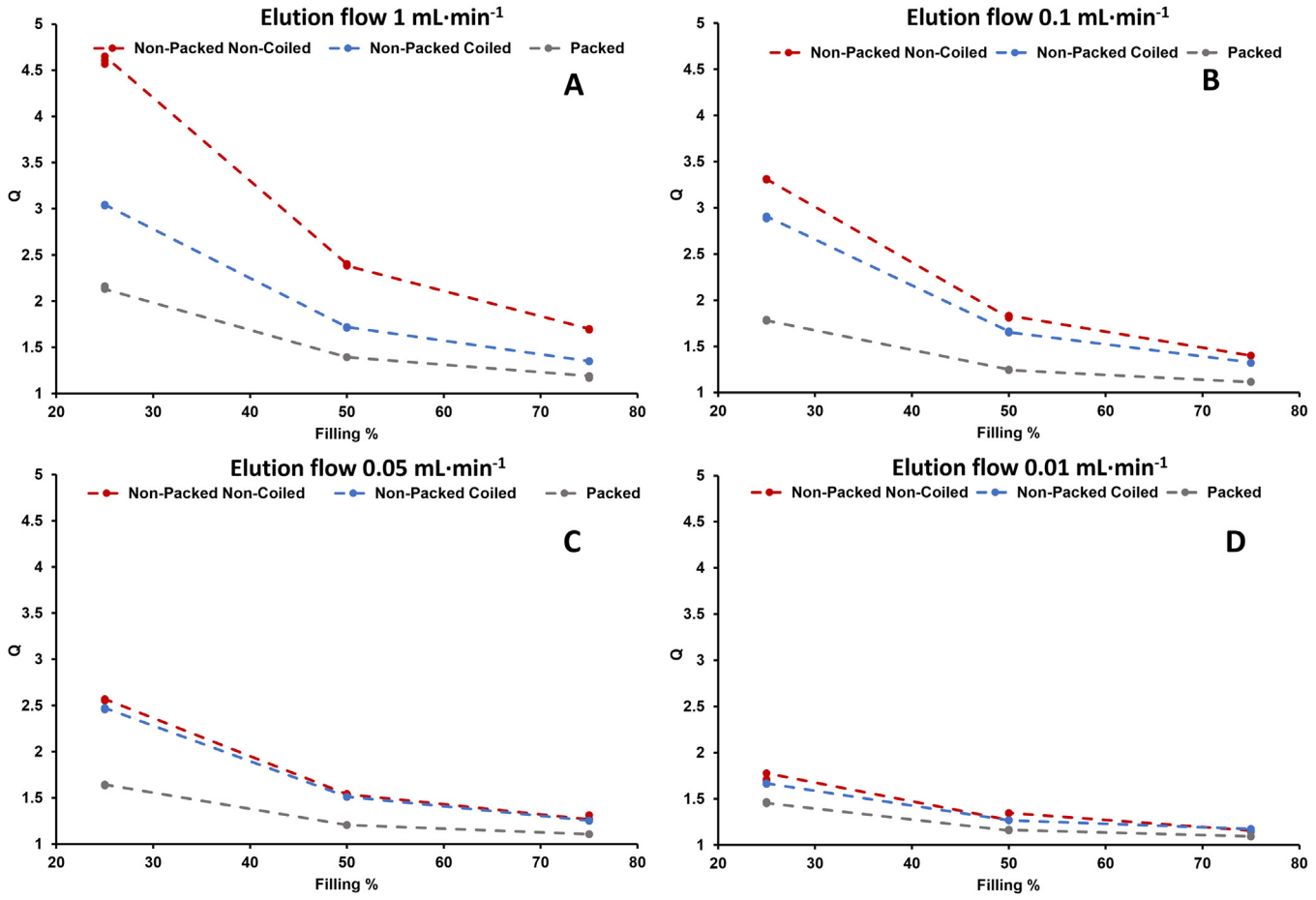

Fig. 4. Ratio of peak broadening between observed and ideal peak (Eq. (8)) for various elution flow rates (1, 0.1, 0.05 and 0.01 mL·min^{-1} for panel A-D respectively) and filling factors in cocurrent elution mode. Dotted lines serve as a visual guide. All data shown represents three repeated measurements.

effect that packing the column has: narrowing the distribution in analyte velocity by increasing radial mixing. Furthermore, packed loops feature a flat velocity profile compared to unpacked loops, further decreasing dispersion. As a pragmatic tool to describe the differences in the observed elution profiles, we used the quotient, Q, of the standard deviation (σ_{observed}, volume), determined using the second moment (μ_2, Eq. (5)), to the ideal injection broadening (σ_{min}, volume, Eq. (1)), as noted in Eq. (8).

$$Q = \frac{\sigma_{\text{observed}}}{\sigma_{\text{min}}} \tag{8}$$

Data was recorded at different elution flow rates and loop filling factors, and the quotient (Eq. (8)) was computed. The resulting data for cocurrent mode is shown in Fig. 4.

The graphs suggests that strongest dispersion effects occur when the loop is emptied at higher flowrates. As flow rates approach the filling flow rate, the differences decrease. At a flow rate of 0.05 mL·min^{-1} (Fig. 4C) the dispersion in the non-packed non-coiled and non-packed coiled loop is practically identical in contrast to the packed loop. The difference in dispersion between the differing filling factors may be attributed to the relative increased contribution of normal longitudinal dispersion effects, as well as the relative increase in the dispersion caused by emptying the loops at a higher flowrate. The dispersion between the different loops becomes relatively similar at 0.01 mL·min^{-1} (Fig. 4D). This is expected as the rate of filling and emptying is identical in these cases causing no additional dispersion to occur.

The skew (S, Eq. (6)) and kurtosis (K, Eq. (7)) were also investigated to compare the elution profiles, and the data is shown in Fig. 5, for elution at 1 mL·min^{-1}. A skew of 0 represents perfect symmetry, whereas a kurtosis of 1.8 represents an ideal block-shaped elution profile (see Supplementary Material Figure S-1). The data in Fig. 5 shows that less tailing was observed for packed and unpacked coiled loops compared to unpacked non-coiled loops with skews closer to 0. Furthermore, the kurtosis was closer to 1.8. The obtained first moment, standard deviation, kurtosis and skew for all experiments performed can be found in Supplementary Material Table S-1.

In countercurrent elution mode (Supplementary Materials Figure S-4) the same effects were observed to a lesser degree. The overall dispersion was reduced and difference between the coiled and non-coiled non-packed loops was already negligible at a 0.1 mL·min^{-1}. Nevertheless, the packed loop featured reduced dispersion in all cases compared to the coiled loops, until a flowrate of 0.01 mL·min^{-1} as was observed in the cocurrent elution mode.

3.2. Investigation of 100 µL loops

As many applications use loops of a larger volume, loops with a volume of 100 µL were also investigated, all experiments were performed at a 50% filling factor and at different elution flow rates. The loops had a larger inner diameter (50 cm × 0.5 mm i.d.) to still maintain a practical loop length. Due to the larger inner diameter (0.5 mm versus 0.25 mm for the 40 µL loop), increased dispersion effects are expected as diffusion across the loop diameter will take more time. Fig. 6 shows a comparison of a non-packed non-coiled, a non-packed coiled and a packed loop. Supplementary Materials Figure S-5 features a version only normalized to peak area.

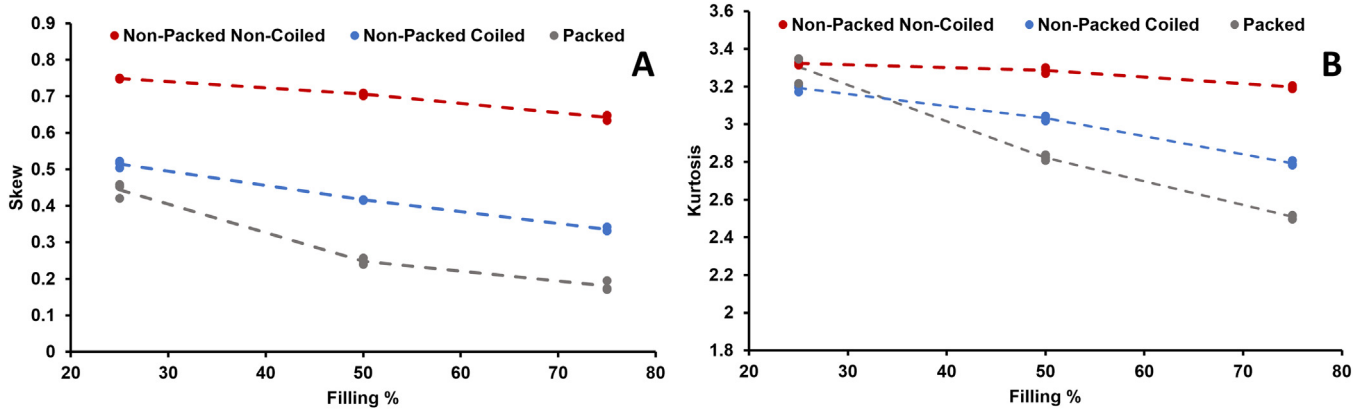

Fig. 5. Mean skew (A) and kurtosis (B) determined for measurements ($n = 3$) at an elution flow rate of 1 mL·min^{-1} and a filling rate of 0.01 mL·min^{-1} given for various filling factors in cocurrent elution mode. Dotted lines serve as a visual guide.

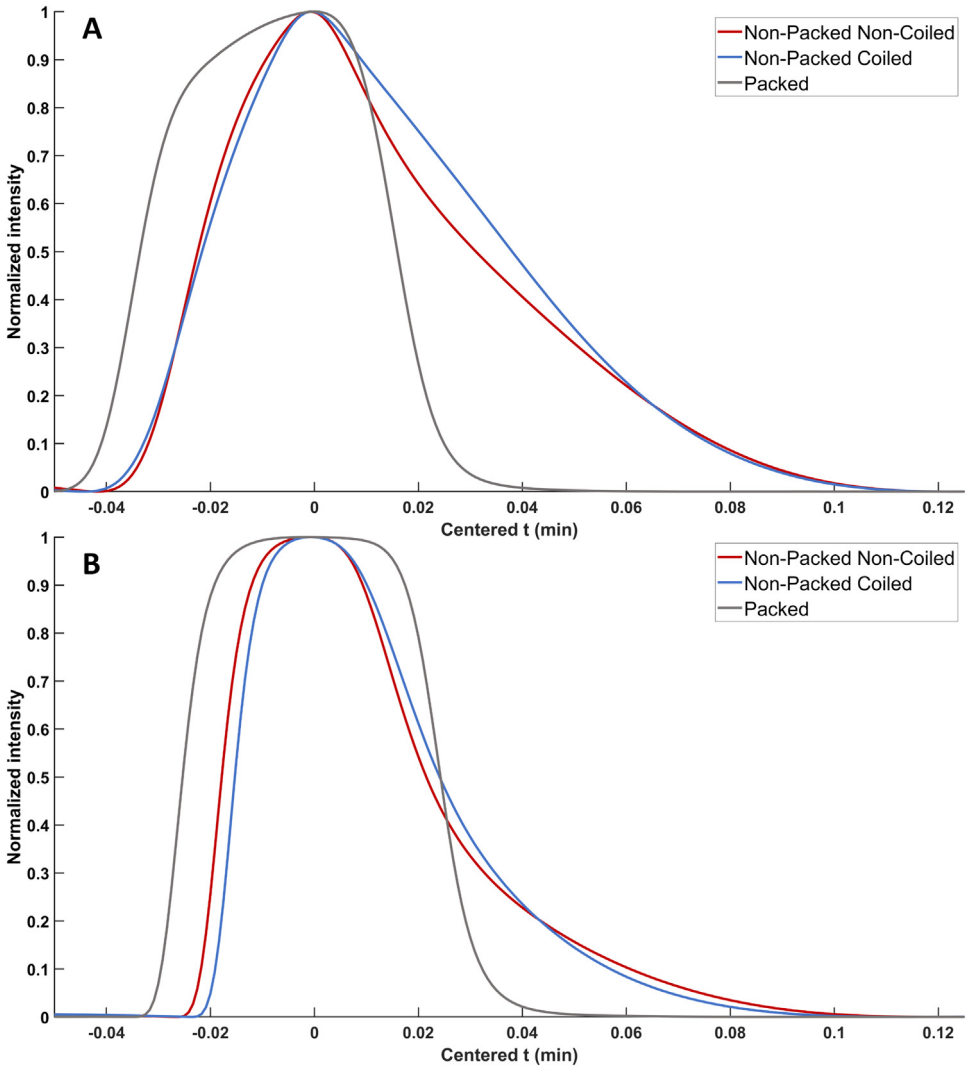

Fig. 6. Mean ($n = 3$) elution profiles of non-packed non-coiled (red), non-packed coiled (blue) and packed loops (grey) in cocurrent (panel A) and countercurrent (B) elution mode both centred and normalized to the peak maximum. Conditions: elution flow rate of 1 mL·min^{-1}, filling rate of 0.01 mL·min^{-1}, filling factor 50%.

As can be seen in Fig. 6 the observed dispersion is again more significant in the cocurrent elution mode (Fig. 6A). In both cases the packed loop features significant reduced dispersion almost yielding a block profile in countercurrent elution. The relative improvement of coiling the loop seems less in these cases, one reason for this could be that there were less coils present in the loop due to it being physically shorter. Another explanation could be that due to the larger inner diameter of the loops coiling does not cause enough mixing to reduce the dispersion significantly. Fig. 7 features the observed dispersion in cocurrent and countercurrent elution modes. The dispersion in the packed loops is nearly constant in all cases indicating that the dispersion is not caused by

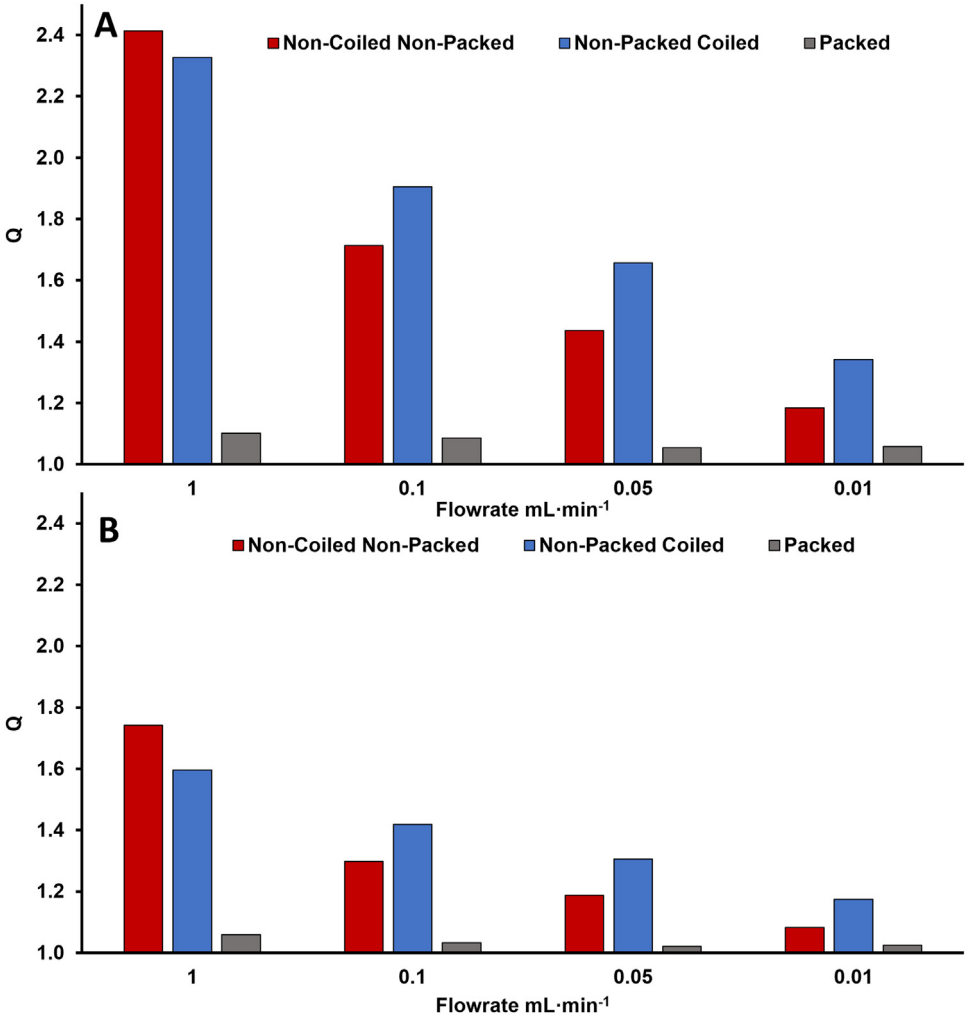

Fig. 7. Average ($n = 3$) peak broadening for various elution flowrates (1, 0.1, 0.05 and 0.01 mL·min^{-1}) at 50% filling (50 µL) in cocurrent (panel A) and countercurrent (panel B) elution mode.

laminar flow effects but rather by normal peak broadening effects, resulting in axial diffusion. While the difference in dispersion between packed and open loops might seem smaller in the 100 µL compared to the 40 µL loops, note that the dispersion is described relative to the injection volume. In Supplementary Materials Figure S-6 the absolute dispersion is given for the examined loops. In general, the absolute dispersion remains relatively constant for the packed loops. In the case of the non-packed loops the absolute dispersion increases with the 100 µL loops, which can be attributed to the larger inner diameter of the loops.

The first moment, standard deviation, skew and kurtosis for the 100 µL loop experiments are given in Supplementary Materials Table S-2. For the packed loop, the skew was closer to 0 (a perfect symmetric profile) under all conditions, which was also true for the kurtosis which always was closer to 1.8 (a perfect block profile).

3.3. Non-aqueous experiments and effect of analyte diffusion

Radial diffusion reduces the dispersion effects observed when analytes elute from conventional unpacked loops. This implies that large analytes such as polymers, which feature very low diffusion coefficients, might benefit more from the use of packed loops. Furthermore, as many separations are not performed under aqueous conditions, experiments under organic conditions are of interest to investigate the application range of packed loops. Therefore, the elution profile of various molar mass polystyrene standards was investigated for the different loop configurations (Section 2.3 for experimental conditions). The experiments were performed on 40 µL loops, in cocurrent elution mode at a filling factor of 50% and an elution flow rate of 1 mL·min^{-1}. Fig. 8 shows a comparison of the non-packed non-coiled, non-packed coiled and packed loops. The effect on the peak width was found to increase significantly compared to the experiments performed under aqueous conditions. The elution profile of the 10 kDa (Fig. 8B) polystyrene standard appears broader than the elution profile obtained for toluene. The artefacts observed at the start of the peaks is caused by the pressure spike from switching the valve and were not included in the assessment of the characteristics of the main peak. The artefacts were likely only visible in the non-aqueous experiments due to the higher compressibility and UV absorbence of THF compared to water [17,18].

Fig. 9 features the quotient of the observed peak width versus the theoretical minimum peak width for various molar masses of polystyrene and toluene. The ratio is reduced in all cases using a packed loop. However, Fig. 9 depicts that high molar mass analytes do not benefit more from the use of a packed loop compared to low molar mass analytes. Although the peak width does increase with molar mass as expected as the molecular diffusion decreases. In the case of the packed loops some additional effects seem to take place, causing the higher molar mass peaks to become asymmetric. Peak profiles of the various molar masses are given

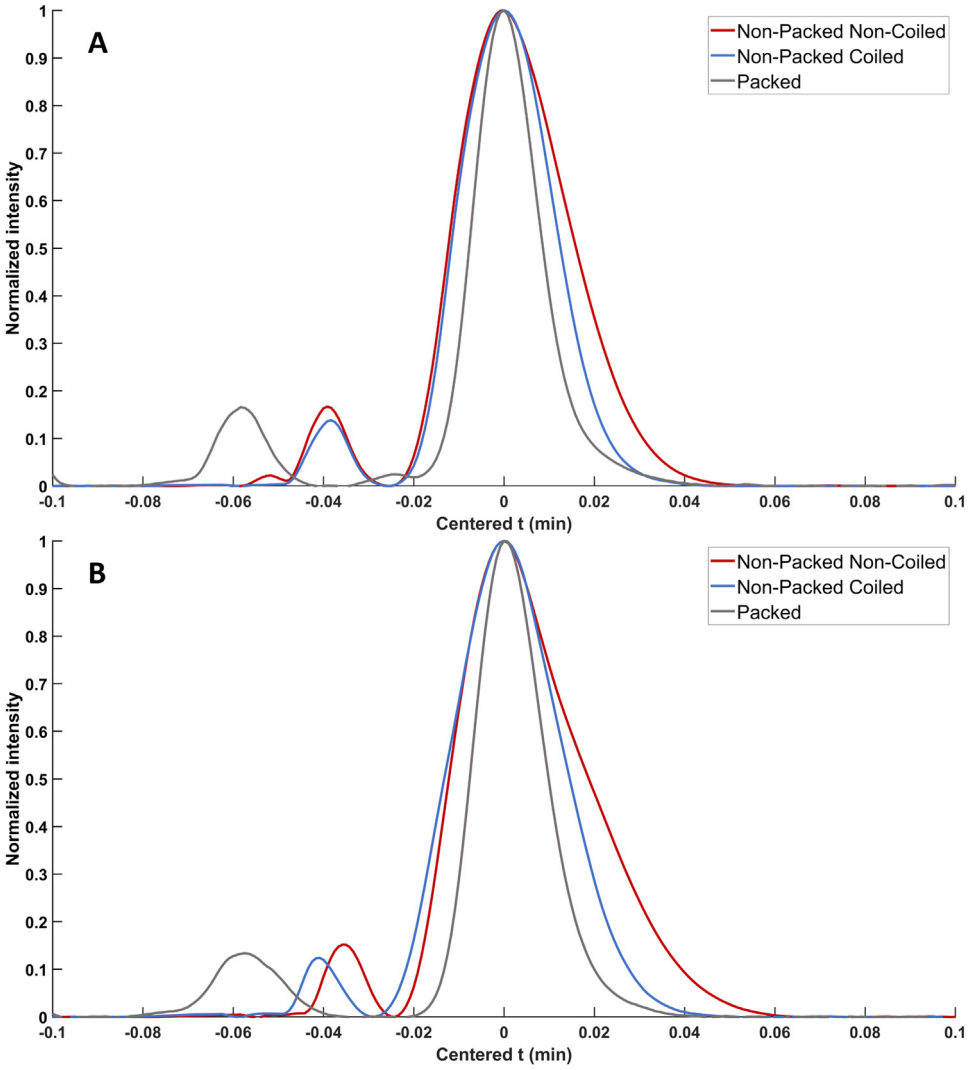

Fig. 8. Mean ($n = 3$) elution profiles of three types of loops filled for 50% at 10 µL·min^{-1} and eluted at 1 mL·min^{-1} in the cocurrent elution mode, panel A features toluene and panel B a 10 kDa polystyrene standard.

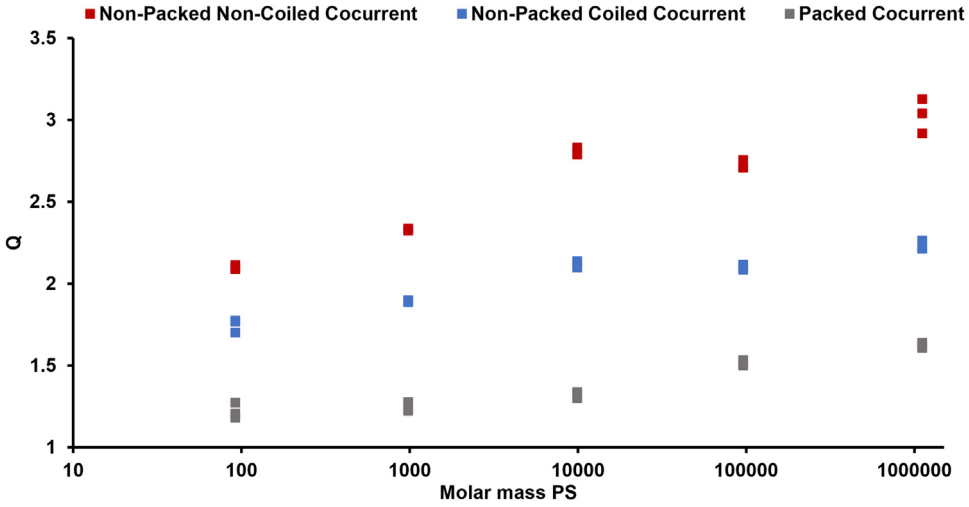

Fig. 9. Peak broadening for the three types of 40µL loops filled for 50% at 10 µL·min^{-1} and eluted at 1 mL·min^{-1} for toluene and various molar masses of polystyrene, performed in triplicate.

in Supplementary Materials Figure S-7. The determination of the exact origins of these effects would require additional studies. As a possible intermediate explanation, since the particles are rather large and non-porous, size-exclusion or hydrodynamic effects are not expected, viscosity effects are more likely to be the origin. High molar mass polymers are render the injected plug more viscous which might result in viscous fingering effects, explaining the peak distortions [19].

4. Conclusion

In this work we found that packed loops are an attractive alternative to conventional unpacked loops in 2D-LC. We found packed loops to yield more desirable elution profiles in all cases. The width of the elution profile (based on the second statistical moment) was closer to the theoretical minimum. Furthermore, the elution profiles were typically more symmetrical (based on the skew) and more similar to the original block profile (based on the kurtosis). These findings were consistent for cocurrent and countercurrent elution modes regardless of loop volume. Our observations did not suggest any significant impact of solvent as our observations under aqueous conditions were also found to be true in an organic solvent. Another benefit of packed loops may be reduction of overfilling, as this is also decreased by introducing more radial diffusion [12,13]. By decreasing the dispersion of emptying the loop and reducing overfilling, a packed loop becomes a more flexible alternative to a conventional unpacked loop.

While improved elution profiles were obtained with packed loops, packing the loops has some downsides. One being the potential for undesired interactions with the stationary phase which could potentially result in loss of analytes or worse elution profiles. The practical implementation of the technique will thus require careful consideration of the analyte, eluent and packing material. In this study non-porous particles were used to reduce the potential for interaction. Besides the use of non-porous particles, the selection of a suitable stationary phase will be critical to the successful implementation of packed loops. Perhaps the most obvious material for the packing beads would be similar to that of the material used for the system components such as the tubing (i.e. PEEK or stainless steel, depending on the application). Alternatively, conventional LC particle technology could be used such as the silica-based particles used in this study. However, in that case it is important to prevent interactions by applying non-porous materials with suitable surface properties regarding the solvent and analytes. Indeed, many considerations can be made regarding suitable packings. Future experimental work will have to demonstrate what materials function best.

Another downside of packed loops is the added pressure, while 20 µm particles were used in this study which theoretically should not yield much pressure (P predicted 42 bar) the frits and narrow connection tubing yielded pressures of 200 bar at 1 $mL{\cdot}min^{-1}$ in water (100 µm packed loops). While undesirable, with modern UHPLC equipment being able to reach pressures of 1200 bar this might not be an issue in practice. Moreover, this could be further reduced with the right selection of frits and packing material. It must also be noted that for our study, the in-house made packed loops were fabricated without the accuracy and quality offered by commercial specialists. Commercial precision would almost certainly yield a much more uniform packing, which might increase the effectiveness and applicability of the method even further.

As mentioned above, packed loops feature some downsides, and our data suggest that coiled loops might suffice in some applications depending on the allowance in the obtained dispersion. Nevertheless, the data also shows that packed loops are capable of yielding further reduced dispersion under a wide range of conditions rendering their implementation of in interest in many 2D-LC applications.

There were many variables in these investigations such as the loop inner diameter, volume, particle size, elution flows, analyte diffusion coefficients etc. Many of these parameters were not optimized. We thus feel that computational studies looking for optimal conditions would be of high interest.

Indeed, our findings essentially emphasize the original concept of packed loops introduced by Coq et al. which surprisingly did not gain traction and its implementation in hyphenated separations thus seems long overdue.

Declaration of Competing Interest

The authors declare that they have no known competing financial interests or personal relationships that could have appeared to influence the work reported in this paper.

CRediT authorship contribution statement

Wouter C. Knol: Conceptualization, Methodology, Investigation, Visualization, Software, Formal analysis, Writing – original draft. **Ron A.H. Peters:** Conceptualization, Supervision, Funding acquisition, Writing – review & editing. **Bob W.J. Pirok:** Conceptualization, Methodology, Supervision, Writing – review & editing.

Data availability

Data will be made available on request.

Acknowledgements

BP acknowledges the project Unleashing the Potential of Separation Technology to Achieve Innovation in Research and Society (UPSTAIRS) (with project number 19173) of the research programme TTW-VENI, which is financed by the Dutch Research Council (NWO). WK acknowledges the UNMATCHED project, which is supported by BASF, Covestro, DSM, and Nouryon, and receives funding from the Dutch Science Council (NWO) in the framework of the Innovation Fund for Chemistry, and from the Ministry of Economic Affairs in the framework of the “PPS-toeslagregeling”. This work was performed in the context of the Chemometrics and Advanced Separations Team (CAST) within the Centre for Analytical Sciences Amsterdam (CASA). The valuable contributions of the CAST members are gratefully acknowledged. The authors would like to thank Prof. Dr. P.J. Schoenmakers and Prof. Dr. Dwight R. Stoll for the useful discussions.

Supplementary materials

Supplementary material associated with this article can be found, in the online version, at doi:10.1016/j.chroma.2023.463802.

References

[1] B.W.J. Pirok, D.R. Stoll, P.J. Schoenmakers, Recent developments in two-dimensional liquid chromatography: fundamental improvements for practical applications, Anal. Chem. 91 (2019) 240–263.
[2] A. Moussa, T. Lauer, D. Stoll, G. Desmet, K. Broeckhoven, Modelling of analyte profiles and band broadening generated by interface loops used in multi-dimensional liquid chromatography, J. Chromatogr. A 1659 (2021) 462578.
[3] S. Tang, C.J. Venkatramani, Resolving solvent incompatibility in two-dimensional liquid chromatography with in-line mixing modulation, Anal. Chem. (2022), doi:10.1021/acs.analchem.2c03572.
[4] D.R. Stoll, K. Shoykhet, P. Petersson, S. Buckenmaier, Active solvent modulation: a valve-based approach to improve separation compatibility in two-dimensional liquid chromatography, Anal. Chem. 89 (2017) 9260–9267.

[5] G. Purcaro, S. Moret, L. Conte, Hyphenated liquid chromatography–gas chromatography technique: recent evolution and applications, J. Chromatogr. A 1255 (2012) 100–111.
[6] W.C. Knol, J.P.H. Smeets, T. Gruendling, B.W.J. Pirok, R.A.H. Peters, Online hyphenation of size-exclusion chromatography and pyrolysis-gas chromatography for polymer characterization, Submitted (2022).
[7] J. Samuelsson, L. Edström, P. Forssén, T. Fornstedt, Injection profiles in liquid chromatography. I. A fundamental investigation, J. Chromatogr. A 1217 (2010) 4306–4312.
[8] S. Deridder, G. Desmet, K. Broeckhoven, Numerical investigation of band spreading generated by flow-through needle and fixed loop sample injectors, J. Chromatogr. A 1552 (2018) 29–42.
[9] E. van Andel, H. Kramers, A. de Voogd, The residence time distribution of laminar flow in curved tubes, Chem. Eng. Sci. 19 (1964) 77–79.
[10] P. Daskopoulos, A.M. Lenhoff, Dispersion coefficient for laminar flow in curved tubes, AIChE J. 34 (1988) 2052–2058.
[11] B. Coq, G. Cretier, J.L. Rocca, M. Porthault, Open or packed sampling loops in liquid chromatography, J. Chromatogr. Sci. 19 (1981) 1–12.
[12] A. Moussa, T. Lauer, D. Stoll, G. Desmet, K. Broeckhoven, Numerical and experimental investigation of analyte breakthrough from sampling loops used for multi-dimensional liquid chromatography, J. Chromatogr. A 1626 (2020) 461283.
[13] B.W.J. Pirok, A.F.G. Gargano, P.J. Schoenmakers, Optimizing separations in online comprehensive two-dimensional liquid chromatography, J. Sep. Sci. 41 (2018) 68–98.
[14] S. Misra, M.F. Wahab, D.C. Patel, D.W. Armstrong, The utility of statistical moments in chromatography using trapezoidal and Simpson's rules of peak integration, J. Sep. Sci. 42 (2019) 1644–1657.
[15] S.R.A. Molenaar, T.A. Dahlseid, G.M. Leme, D.R. Stoll, P.J. Schoenmakers, B.W.J. Pirok, Peak-tracking algorithm for use in comprehensive two-dimensional liquid chromatography – application to monoclonal-antibody peptides, J. Chromatogr. A 1639 (2021) 461922.
[16] Y. Wu, Z. Fan, Y. Lu, Bulk and interior packing densities of random close packing of hard spheres, J. Mater. Sci. 38 (2003) 2019–2025.
[17] X. Zhou, N. Furushima, C. Terashima, H. Tanaka, M. Kurano, New micro-flow pumping system for liquid chromatography, J. Chromatogr. A 913 (2001) 165–171.
[18] S.E. Walker, R.A. Mowery, R.K. Bade, LC Solvents and spectral considerations with a new process liquid chromatographic optical absorbance detector, J. Chromatogr. Sci. 18 (1980) 639–649.
[19] K.J. Mayfield, R.A. Shalliker, H.J. Catchpoole, A.P. Sweeney, V. Wong, G. Guiochon, Viscous fingering induced flow instability in multidimensional liquid chromatography, J. Chromatogr. A 1080 (2005) 124–131.